Research on Engineering Structures & Materials
www.jresm.org

Research Article

Performance analysis of fuzzy-LQR and fuzzy-LQG controllers for active vehicle suspension systems

Emre Kemer*[1,a], Hasan Başak[2,b]

[1]*Faculty of Eng. and Natural Sciences, Electrical-Electronics Eng., Uşak University, Uşak, Türkiye*
[2]*Faculty of Eng., Electrical-Electronics Eng., Artvin Çoruh University, Artvin, Türkiye*

Article Info

Article history:

Received 07 Feb 2024
Accepted 14 Apr 2024

Keywords:

FLQR control;
FLQG control;
Road disturbance;
Ride comfort;
Quarter-car suspension system

Abstract

Suspension systems in vehicles are crucial to both ride quality and driving security. The challenge of creating an effective control mechanism for automotive active suspension systems is addressed in this work. In the event of unforeseen road disturbances, the active suspension systems are intended to deliver a more pleasant ride and good handling. Fuzzy-Linear Quadratic Gaussian (FLQG) and Fuzzy-Linear Quadratic Regulator (FLQR) controllers adapting to road disturbances are proposed to enhance vehicle comfort through the reduction of the driver's overall body acceleration. The simulation findings demonstrate that the FLQR and FLQG controllers are efficient in adjusting the automotive suspension configuration under varying road profiles compared to those of the conventional LQR and LQG controllers.

1. Introduction

The suspension systems of vehicles maintain the wheels in a near position with the chassis while travelling. The currently available vehicle suspension technology can be categorized as active, semi-active and passive suspension systems. Energy absorption in passive suspensions reduces road impacts without active control, while semi-active suspensions offer dynamic adjustments to stiffness or damping, optimizing flexibility across different road surfaces [1]. An actuator in the active suspension system introduces additional forces between the tires and the vehicle, implementing an active control strategy. This system creates adjustable suspension control forces to guarantee that the vehicle's handling is smooth and stable [2]. Active suspension systems in vehicles aim to ensure ride comfort, road holding, and passenger safety for different road irregularities. To utilize the potential of active suspension systems, the control algorithms should deal with changing road profiles. The control objectives of active suspension systems are passenger comfort, minimum vehicle body acceleration, and road handling. In the literature, various control algorithms have been designed for active suspension systems. Adaptive control [3] enables the suspension system to adapt its parameters in real-time based on feedback signals, thus ensuring adaptability to changing road conditions and vehicle dynamics. However, adaptive control suffers from computational complexity and tuning challenges. Sliding mode control [4,5], employs discontinuous control laws to provide robust performance in the presence of uncertainties and disturbances. Nevertheless, it can exhibit chattering phenomena and require careful design to mitigate undesirable effects. Despite efforts to address chattering, the phenomenon may still affect the stability of the system. Therefore,

*Corresponding author: emre.kemer@usak.edu.tr
[a] orcid.org/ 0000-0001-8716-1971; [b] orcid.org/0000-0002-3724-6819
DOI: http://dx.doi.org/10.17515/resm2024.177ce0207rs

combining sliding mode control with PI/PID and fuzzy control can be addressed to obtain a control algorithm that can manage chattering while ensuring stable and robust performance [6, 7]. Model predictive control [8], utilizes predictive models of vehicle dynamics to generate optimal control actions over a finite time horizon, offering precise control while considering future system states and constraints. However, model predictive control may entail high computational demands and require accurate models for effective implementation. Fuzzy control [9] utilizes linguistic variables and fuzzy rules to achieve adaptive and intuitive control of suspension systems. Fuzzy control may lack robustness in handling uncertainties and external disturbances. Therefore, H_∞ control theory combines fuzzy logic to achieve robust performance and disturbance rejection [10]. Yet, it may introduce complexity in controller design and tuning due to the integration of multiple control strategies. PID controller based on the genetic algorithm [8] offers a straightforward yet effective approach to suspension control. Nonetheless, PID controllers exhibit limited adaptability to varying operating conditions. Adaptive fuzzy PID control [9] integrates fuzzy logic with PID control to enhance adaptability and robustness. However, it suffers from complexity in design and tuning due to the combination of multiple control techniques. A state feedback optimal control law namely Linear Quadratic Regulator (LQR) is designed to obtain optimal performance without deteriorating conflict design requirements [11,12]. LQR offers guaranteed stability, robustness, and a structured design method for multiple-input multiple-output systems. The LQR approach computes an optimal state-feedback gain by minimizing a quadratic performance index, which consists of the state and input variables penalized by the weighting matrices. Linear Quadratic Gaussian (LQG) control [13] combines optimal control theory with state estimation techniques to design controllers that minimize a quadratic cost function while accounting for uncertainties and noise.

Fuzzy logic can capture the complex and nonlinear relationships inherent in suspension dynamics. By encoding expert knowledge and linguistic variables into fuzzy rule sets, fuzzy logic enables the controller to make intuitive and adaptive decisions in response to varying road conditions. On the other hand, LQR and LQG controllers provide robust mathematical frameworks for optimal control design. These controllers leverage system models and performance criteria to synthesize control laws that minimize the system's performance such as ride comfort and handling stability. In this study, Fuzzy-LQR (FLQR) and Fuzzy–LQG (FLQG) controllers are proposed for enhancing the performance of the active suspension system. FLQR and FLQG approaches integrate the adaptive and intuitive decision-making capabilities of fuzzy logic with the rigorous optimization principles of LQR and LQG control. This combination enables the controller to effectively adapt to changing operating conditions while optimizing the system's performance. The developed fuzzy controllers are evaluated by comparing their performances with those of the standard LQR and LQG controllers in terms of vehicle body acceleration, suspension deflection, and tire deflection. Simulation results have shown that the designed fuzzy controllers can achieve better closed-loop responses.

The structure of the remaining article is as follows: Section 2 introduces the model of an active suspension system, followed by the development of FLQR and FLQG controllers in Section 3. Section 4 gives simulation results and provides a discussion of the outcomes, and Section 5 gives the conclusions of the paper.

2. Material and Method

2.1. Quarter Active Suspension System

This section outlines the dynamic equations that govern the behavior of a quarter-active suspension system. The quarter active suspension system is depicted in Fig. 1. The system has two inputs (control input F and the road surface position, z_r). The vehicle body displacement and the tire displacement are denoted by z_s and z_{us} from the ground respectively.

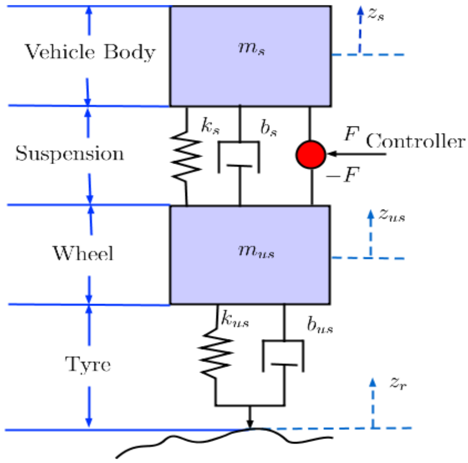

Fig. 1. Diagram of the quarter active vehicle suspension system

The quarter active suspension system equations of motion are derived in [14] using the Newton law as follows:

$$m_{us}\ddot{z}_{us} = -b_{us}\dot{z}_{us} - b_s\dot{z}_{us} - F + b_s\dot{z}_s + b_{us}\dot{z}_r - (z_{us} - z_s)k_s - (z_{us} - z_r)k_{us} \tag{1}$$

$$m_s\ddot{z}_s = b_s\dot{z}_{us} + F - b_s\dot{z}_s - (z_s - z_{us})k_s \tag{2}$$

Eqs. (1)-(2) can be given in the state–space realization as:

$$\begin{aligned}\dot{x}(t) &= \mathcal{A}x(t) + \mathcal{B}u(t)\\ y(t) &= \mathcal{C}x(t) + \mathcal{D}u(t)\end{aligned} \tag{3}$$

where the state variable vector is $x = [x_1 \quad x_2 \quad x_3 \quad x_4] = [(z_s - z_{us})\ \dot{z}_s\ (z_{us} - z_r)\ \ \dot{z}_{us}]^T$ and the input vector is $u = [\dot{z}_r \ \ F\,]^T$ and the output vector is $y = [\,(z_s - z_{us})\ \ \ddot{z}_s\,]^T$. $(z_s - z_{us})$ and $(z_{us} - z_r)$ are the suspension and tire deflections, $\dot{z}_s$ and $\dot{z}_{us}$ are the body and the tire vertical velocities respectively. The following matrices are obtained:

$$\mathcal{A} = \begin{bmatrix} 0 & 1 & 0 & -1 \\ \frac{-k_s}{m_s} & \frac{-b_s}{m_s} & 0 & \frac{b_s}{m_s} \\ 0 & 0 & 0 & 1 \\ \frac{k_s}{m_{us}} & \frac{b_s}{m_{us}} & \frac{-k_{us}}{m_{us}} & -\frac{(b_s+b_{us})}{m_{us}} \end{bmatrix}, \quad \mathcal{B} = \begin{bmatrix} 0 & 0 \\ 0 & \frac{1}{m_s} \\ -1 & 0 \\ \frac{b_{us}}{m_{us}} & -\frac{1}{m_{us}} \end{bmatrix}, \tag{1}$$

$$\mathcal{C} = \begin{bmatrix} 1 & 0 & 0 & 0 \\ \frac{-k_s}{m_s} & \frac{-b_s}{m_s} & 0 & \frac{b_s}{m_s} \end{bmatrix}, \quad \mathcal{D} = \begin{bmatrix} 0 & 0 \\ 0 & \frac{1}{m_s} \end{bmatrix}.$$

Table 1 provides the specifications of the quarter active suspension system.

Table 1. Model parameters [14]

Symbol	Value	Definition
m_s	2.45 kg	Sprung Mass
m_{us}	1 kg	Unsprung Mass
k_s	900 N/m	Suspension Stiffness
k_{us}	1250 N/m	Tire Stiffness
b_s	7.5 Ns/m	Suspension Inherent Damping coefficient
b_{us}	5 Ns/m	Tire Inherent Damping coefficient

2.1.1 Performance Requirements

The active suspension system's performance criteria are given in [15] as:

1) Ride comfort: The vehicle body acceleration $\ddot{z}_s$ must be reduced by the active suspension system.

2) Suspension deflection: The active suspension system has to maintain the suspension deflection within the allowable interval to avoid vehicle damage. $|(z_s - z_{us})| \leq \bar{z}$, $\bar{z}$ is the greatest acceptable suspension deflection ($\bar{z} = 0.038$).

3) Road handling: The wheel assembly has to stay in firm contact with the road to ensure passenger safety. Therefore, the tire's dynamic load has to be smaller than its static load ($|k_s(z_{us} - z_r)| \leq (m_s + m_{us})g$).

3. Fuzzy-LQR and Fuzzy-LQG Controller Development

3.1. LQR Control

Consider the following linear time-invariant system:

$$\dot{x}(t) = \mathcal{A}x(t) + \mathcal{B}u(t), \qquad x(0) = x_0 \tag{5}$$
$$y(t) = \mathcal{C}x(t) + \mathcal{D}u(t)$$

in which $x(0)$ is the initial condition. The purpose is to find the optimal control law, $u(t)$ which can drive the state variables of the dynamics to demand ones by optimizing the following equation:

$$J = \int_0^\infty x^T(t)Qx(t) + u^T(t)\mathcal{R}\,u(t)dt, \tag{6}$$

Here Q is the positive semi-definite and $\mathcal{R}$ is the positive-definite weighting matrices. Diagonal weighting matrices are generally selected. The order of Q and $\mathcal{R}$ matrices are equal to the number of states and inputs. Bryson's rule is used to obtain acceptable Q and $\mathcal{R}$ matrices in the literature. Initially $Q = I$ and $\mathcal{R} = \gamma I$ can be used. Assume that $(\mathcal{A}, \mathcal{B})$ is stabilisable and $(\mathcal{A}, \mathcal{C})$ is observable, then the LQR controller computes as follows:

$$u(t) = -Kx(t) \tag{7}$$

in which K is the optimal state-feedback gain computed by $K = \mathcal{R}^{-1}\mathcal{B}^T\mathcal{P}$ that is called the Lagrange multiplier based on optimization. The positive definite-matrix, $\mathcal{P}$ is obtained from the solution of the following Algebraic Riccati Equation [16]:

$$\mathcal{A}^T\mathcal{P} + \mathcal{P}\mathcal{A} + Q - \mathcal{P}\mathcal{B}\mathcal{R}^{-1}\mathcal{B}^T\mathcal{P} = 0 \tag{8}$$

3.2. Fuzzy-LQR Control

Fuzzy-LQR controller consists of an LQR control and a fuzzy control. The FLQR control structure is given in Fig. 2. A linear fusion function is used including error (E) and error change (EC) which reduces the number of rules for the fuzzy logic control [17]. The linear fusion function, $F_1(X)$ is given as follows.

$$F_1(X) = \begin{vmatrix} K_{x_1} & 0 & K_{x_3} & 0 \\ 0 & K_{x_2} & 0 & K_{x_4} \end{vmatrix} \tag{2}$$

and E and EC are computed as:

$$\begin{vmatrix} E \\ EC \end{vmatrix} = F_1(X) \begin{vmatrix} x_1 \\ x_2 \\ x_3 \\ x_4 \end{vmatrix} \tag{3}$$

$$\begin{aligned} E &= K_{x_1}\, x_1 + K_{x_3} x_3 \\ EC &= K_{x_2} x_2 K_{x_4}\, x_4 \end{aligned} \tag{4}$$

Here, the purpose of developing the Mamdani-type fuzzy model is to set the closed-loop state-feedback gains. The transformation of the input variables (E and EC) and the output variable (Fc) into linguistic variables is performed as: (ZE-zero error, PS-positive small, PM-positive medium, PB-positive big, NB-negative big, NM-negative medium, NM-negative small) [18]. The fuzzy rules of the controller are given in Table 2. As can be seen from the table, there exist 49 rules which are implemented to control the active suspension system.

Table 2. Fuzzy Logic Rules

E				**EC**			
	NB	NM	NS	ZE	PS	PM	PB
NB	NB	NB	NB	NM	NM	NS	ZE
NM	NB	NB	NB	NM	NS	ZE	PS
NS	NS	NM	NM	NS	ZE	PS	PM
ZE	NM	NM	NS	ZE	PS	PM	PB
PS	NM	NS	ZE	PS	PM	PM	PB
PM	NS	ZE	PS	PM	PM	PB	PB
PB	ZE	PS	PM	PM	PB	PB	PB

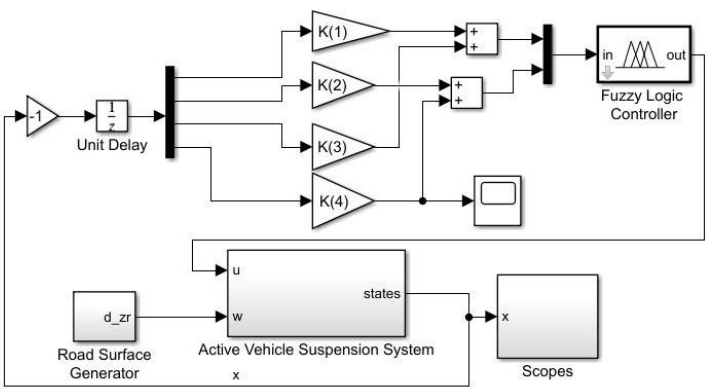

Fig. 2. FLQR control structure

The input variables, E and EC vary in intervals [-10 10 cm]. The output variable changes in the interval [-38.5 38.5 N]. The input and output variables are inferred graphically using triangular membership functions. Figs. 3, 4 and 5 illustrate the membership of the input and output variables. The relationship between the FLC's inputs and outputs is depicted in Fig. 6

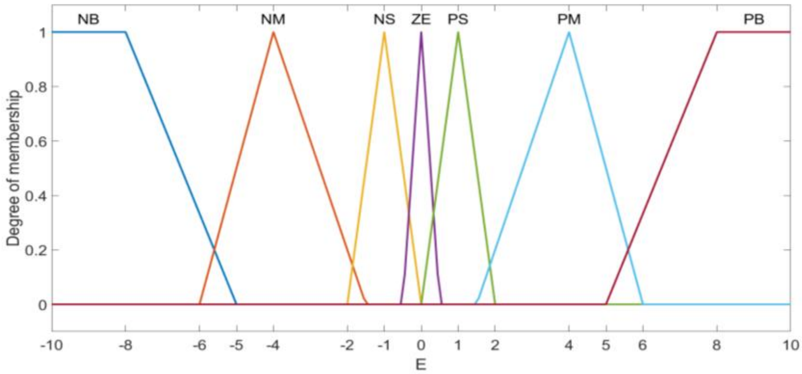

Fig. 3. The membership functions of the input variable, E

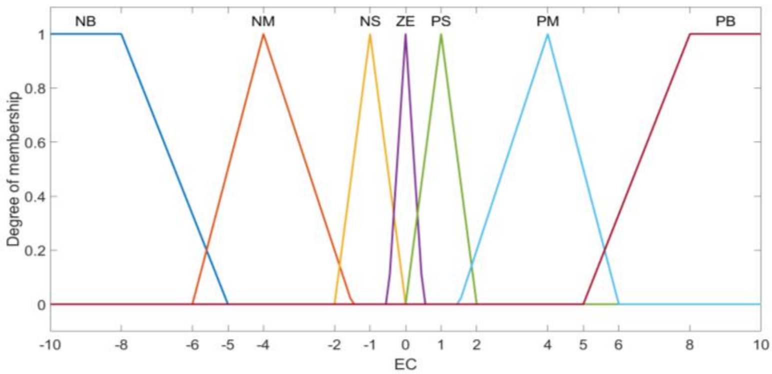

Fig. 4. The membership functions of the input variable, EC

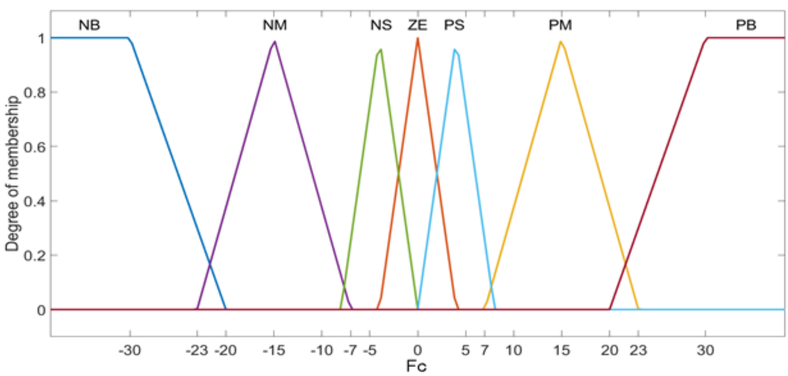

Fig. 5. The membership functions of the input variable, Fc

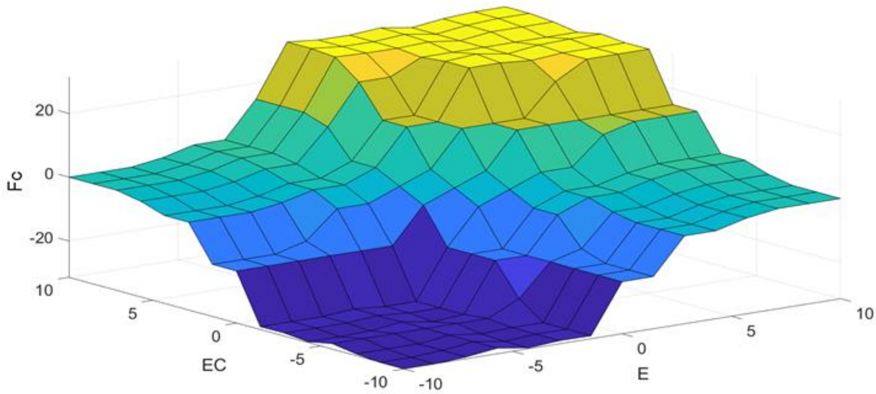

Fig. 6. Fuzzy logic surface

3.3. Fuzzy-LQG Control

In the LQR control design, all states are assumed to be available. This assumption is not valid in practice. Kalman filter (Fig. 7) estimates the system states from the information of input and output in Fig. 8. The state space model of the active suspension system with the zero mean Gaussian white noise is given as follows:

$$\begin{aligned} \dot{x}(t) &= \mathcal{A}x(t) + \mathcal{B}u(t) + n_d \\ y(t) &= \mathcal{C}x(t) + n_y \end{aligned} \tag{5}$$

where the pair $(\mathcal{A}, \mathcal{C})$ is detectable, and the pair of $(n_{\mathrm{d}}, n_{\mathrm{y}})$ represents white noise satisfies that

$$E[n_d\, {n_d}^T] = \tilde{Q},\, E[n_y\, {n_y}^T] = \tilde{R} \quad and \quad E[n_d\, {n_y}^T] = 0 \tag{6}$$

with $\tilde{Q} \geq 0$ and $\tilde{R} > 0$. Let $\tilde{P}$ satisfy the following Riccati equation.

$$\mathcal{A}^T \tilde{P} + \tilde{P}\mathcal{A} + \tilde{Q} - \tilde{P}\,\mathcal{C}^T \tilde{R}^{-1} \mathcal{C}\,\tilde{P} = 0 \tag{7}$$

Kalman filter is given as following dynamic equations:

$$\begin{aligned} \dot{\hat{x}}(t) &= \mathcal{A}\hat{x}(t) + \mathcal{B}u(t) + K_F(y - \hat{y}) \\ y(t) &= \mathcal{C}\hat{x}(t) \end{aligned} \tag{8}$$

Where;

$$K_F = \tilde{P}\mathcal{C}^T \tilde{R}^{-1} \tag{9}$$

Kalman filter minimizes the prediction of the error covariance when presumed conditions are met [19].

FLQG controller is obtained by combining the LQG controller and fuzzy logic controller as shown in Fig. 9. Kalman filter estimates the state variables using the input and measured output variables of the active suspension system. The estimated variables can be used for the FLQR which completes the design of the FLQG given in Fig. 9. The simulation results will be given in the next section.

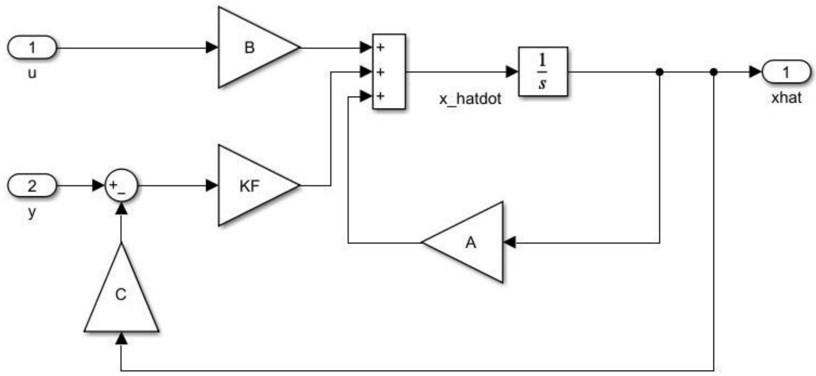

Fig. 7. The structure of the Kalman filter

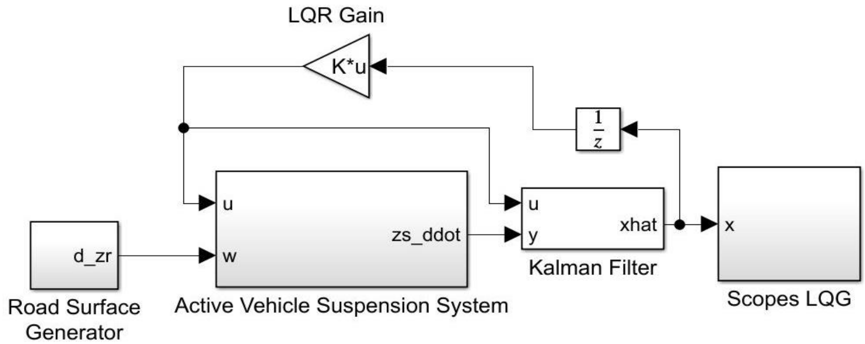

Fig. 8. LQG control structure of the active vehicle suspension system

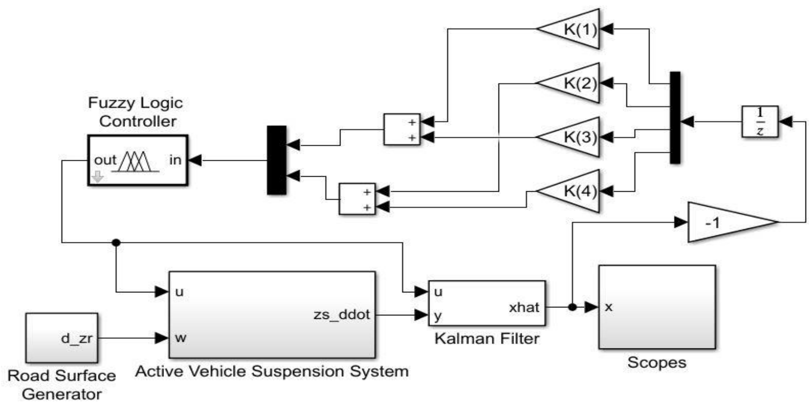

Fig. 9. FLQG control structure of the active vehicle suspension system

4. Simulation Results and Discussion

This section presents simulation results to show the effectiveness of the active suspension system with the FLQR and the FLQG controllers against random road disturbances. Two cases of road disturbances are taken into consideration as follows: Case 1 is a square signal with an amplitude of 0.01 m and frequency of 0.3 Hz. Case 2 is a chirp signal, which begins at a frequency of 1Hz and an amplitude of 0.0015 m, which reaches a frequency of 8 Hz at

25s. The FLQR and the FLQG controllers are compared with the conventional LQR and LQG controllers under the mentioned road disturbances.

Fig. 10(a) compares the vehicle body acceleration closed-loop responses for the square road profile. It can be seen that the FLQR controller (green line) provides lower body acceleration than the conventional LQR does. To void structural damage, the absolute value of the suspension deflection should be less than 0.038 m ($|(z_s - z_{us})| \leq 0.038$ m). Figs. 10(b) and 10(c) display the vehicle suspension and tire deflections respectively. Fig. 10(a) also compares the vehicle body acceleration closed-loop responses with the LQG and FLQG controllers. It can be seen that the FLQG controller (red dashed line) obtains a body acceleration, 0.055 m/s^2 which is lower than the result of the conventional LQG controller. The vehicle suspension and tire deflection results of the LQG and FLQG controller are seen in Figs. 10(b) and 10(c) respectively. The results of suspension deflections with controllers provide that $|(z_s - z_{us})| \leq 0.015$ m which is within the acceptable range. For road handling requirements, the tire's dynamic load has to be smaller than its static load ($(m_s + m_{us})g = 33.84\ N$). All controllers satisfy this performance requirement. More precisely, the active suspension system with the classical LQR and LQG controllers has tire's dynamic load, $|k_s(z_{us} - z_r)| = 8.6\ N$ and $7.7\ N$ respectively. The maximum tire's dynamic loads of the active suspension system with the FLQR and FLQG controllers are 8.57 N and *7.6* N respectively*.* As a result, the FLQR and FLQG controllers have a dynamic load within the permissible range.

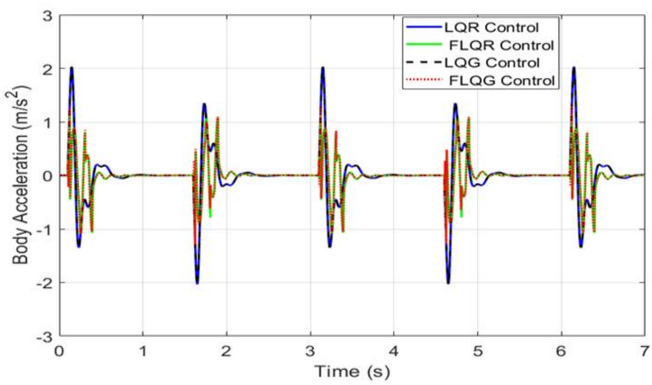

(a)

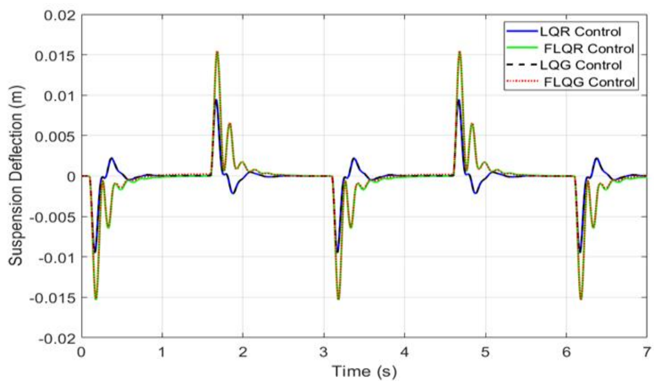

(b)

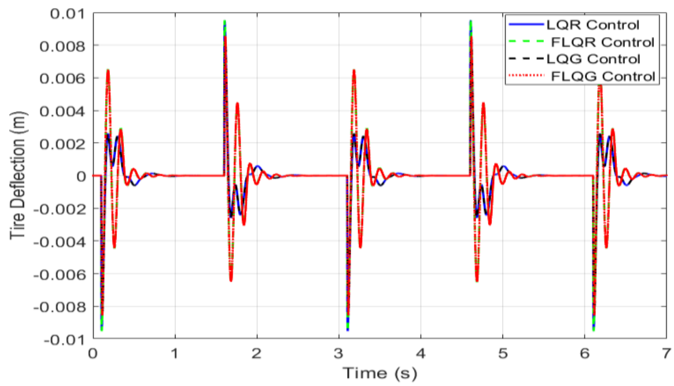

(c)

Fig. 10. Comparison of closed-loop responses (Case 1)

Next, test results of controllers in the presence of chirp road disturbance are given as follows. Closed-loop responses are given in Fig.11. Vehicle body vertical acceleration plots are given in Fig.10(a) to evaluate the passenger ride comfort. The FLQR provides an improvement of *70%* over the conventional LQR controller and the FLQG controller has an improvement of *75.5%* over the conventional LQG controller. Fig. 11(b) indicates the suspension deflection. The LQR controller increases the suspension deflection to improve ride comfort. The FLQR and FLQR controllers having the maximum value of the suspension deflection are 0.002 m and 0.0019 m respectively, which are less than the permissible travel range of 0.038 m. Lastly, the tire deflection is depicted in Fig. 11(c). The dynamic loads with LQR, FLQR, LQG and FLQG controllers are 1.04 N, 0.37 N, 0.96 N and 0.33 N respectively, which are lower than the tire's static load. Furthermore, the FLQG controller achieves the best tire deflection amongst all designed controllers. The FLQR and FLQG controllers reduce the suspension in the presence of chirp road disturbance. Root-mean-square (RMS), minimum (Min), maximum (Max) and peak-to-peak values are reported in Table 3 under the square road condition. Closed-loop responses with the FLQR and FLQG controllers achieve the lowest RMS indices.

Table 3. Statistical analysis of the body acceleration with different controllers (Case 1)

Controller	LQR	Fuzzy-LQR	LQG	Fuzzy-LQG
Max	2.029	**1.141**	2.029	**1.291**
Min	-2.029	**-1.138**	-2.029	**-1.286**
Peak to Peak	4.058	**2.279**	4.058	**2.576**
RMS	0.4648	**0.2839**	0.4658	**0.2844**

Furthermore, statistical analysis of the body acceleration with the FLQR and the FLQG controllers under the chirp road disturbance is given in Table 4. According to Table 4, the FLQR and the FLQG controllers improve the performance of the active suspension system. Simulation and statistical results show that the fuzzification of the LQR and LQG controllers improves ride comfort and reduces suspension and tire deflections under different road disturbances.

Table 4. Statistical analysis of the body acceleration with different controllers (Case 2)

Controller	LQR	Fuzzy-LQR	LQG	Fuzzy-LQG
Max	0.4729	**0.2055**	0.475	**0.1905**
Min	-0.4646	**-0.1984**	-0.4667	**-0.1892**
Peak to Peak	0.9374	**0.404**	0.9416	**0.3797**
RMS	0.2027	**0.05218**	0.2037	**0.05263**

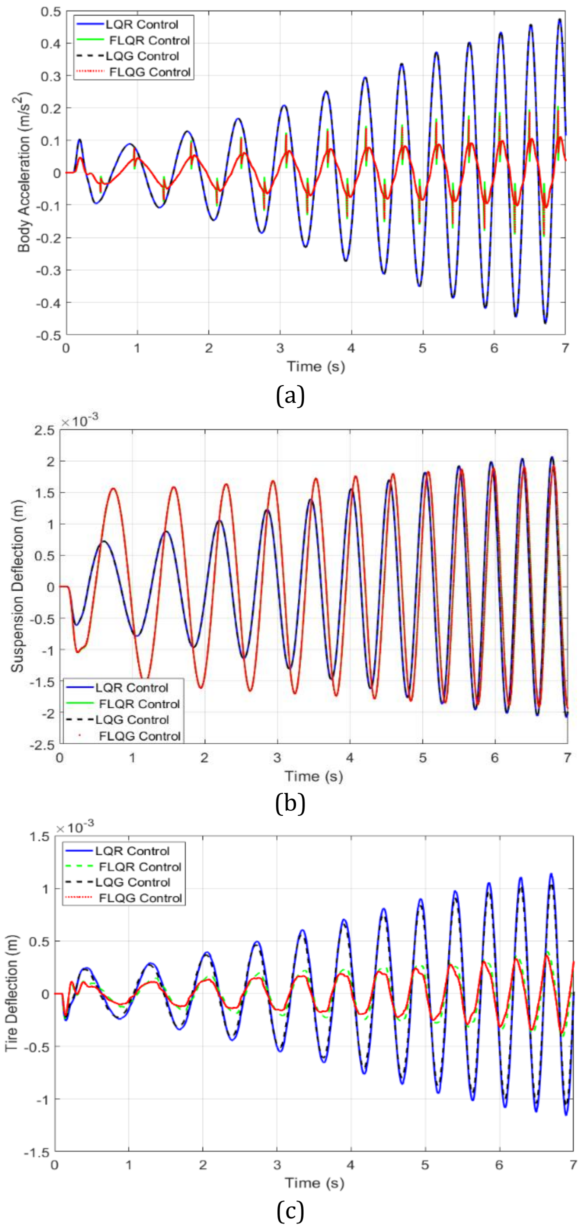

Fig. 11. Comparison of closed-loop responses (Case 2)

5. Conclusions

The active suspension system of a vehicle plays a crucial role in evaluating dynamic performance metrics such as ride comfort, road handling, and suspension deflection. Enhancing ride comfort and handling stability in active suspension systems relies heavily on the effectiveness of the active suspension controller. Thus, this study focuses on the development of Fuzzy-LQR and Fuzzy-LQG control approaches for active suspension systems, specifically targeting the active quarter suspension system without considering road input signals.

Using the active quarter suspension system as the study subject, Fuzzy-LQR and Fuzzy-LQG controllers were designed independently of road input signals. Simulation studies were conducted using the Matlab/Simulink environment to evaluate the performance of these controllers. Comparative analysis was performed against both passive suspension and active suspension systems employing standard LQR/LQG control approaches.

Simulation results demonstrate the efficacy of Fuzzy-LQR and Fuzzy-LQG controllers in improving ride quality compared to standard LQR and LQG controllers. The fuzzy controllers effectively reduce vehicle body acceleration while maintaining permissible suspension deflection in the presence of road disturbances. Specifically, the Fuzzy-LQR and Fuzzy-LQG controllers reduce the root mean square (RMS) values of vertical body acceleration in the presence of square road disturbances by 38.7% and 38.9%, respectively. Moreover, in the presence of chirp road disturbances, the Fuzzy-LQR and Fuzzy-LQG controllers achieve even greater reductions, lowering RMS values of vertical body acceleration by 73.9% and 74.25%, respectively.

Future research directions will focus on experimental validation of the proposed controllers, addressing several key points. Firstly, the application of the suggested control mechanisms will be extended to nonlinear active suspension systems to provide a more accurate representation of genuine suspension dynamics. Secondly, efforts will be directed towards developing fuzzy controllers for dynamic models encompassing entire car active suspensions, with the ultimate goal of implementing these controllers in real-world suspension systems. This emphasis on experimental validation will contribute to bridging the gap between theoretical advancements and practical implementation, enhancing the overall effectiveness and applicability of active suspension control strategies.

References

[1] Tang L, Ren NL and Funkhouser S. Semi-active Suspension Control with PSO Tuned LQR Controller Based on MR Damper. International Journal of Automotive and Mechanical Engineering, 2023; 20(2): 10512-10522. https://doi.org/10.15282/ijame.20.2.2023.13.0811

[2] Hua C, Chen J, Li Y, and Li L. Adaptive prescribed performance control of half-car active suspension system with unknown dead-zone input. Mechanical Systems and Signal Processing, 2018; 111: 135-148. https://doi.org/10.1016/j.ymssp.2018.03.048

[3] Fialho I, Balas GJ. Road adaptive active suspension design using linear parameter-varying gain-scheduling. IEEE Trans. Control Syst. Technol., 2002; 10(1): 43-54. https://doi.org/10.1109/87.974337

[4] Deshpande VS, Mohan B, Shendge PD and Phadke SB. Disturbance observer based sliding mode control of active suspension systems. J. Sound Vib., 2014; 333 (11): 2281-2296. https://doi.org/10.1016/j.jsv.2014.01.023

[5] Nguyen DN, Nguyen TA. Evaluate the stability of the vehicle when using the active suspension system with a hydraulic actuator controlled by the OSMC algorithm. Scientific reports, 2022; 12(1): 19364. https://doi.org/10.1038/s41598-022-24069-w

[6] Nguyen DN, Nguyen TA. Proposing an original control algorithm for the active suspension system to improve vehicle vibration: Adaptive fuzzy sliding mode proportional-integral-derivative tuned by the fuzzy (AFSPIDF). Heliyon, 2023; 9(3). https://doi.org/10.1016/j.heliyon.2023.e14210

[7] Nguyen TA. A novel approach with a fuzzy sliding mode proportional integral control algorithm tuned by fuzzy method (FSMPIF). Scientific Reports, 2023; 13(1): 7327. https://doi.org/10.1038/s41598-023-34455-7

[8] Papadimitrakis M, Alexandridis A. Active vehicle suspension control using road preview model predictive control and radial basis function networks. Applied soft computing, 2022; 120: 108646. https://doi.org/10.1016/j.asoc.2022.108646

[9] Cao J, Li P, and Liu H. An interval fuzzy controller for vehicle active suspension systems. IEEE Trans. Intell. Transp. Syst., 2010; 11(4): 885-895. https://doi.org/10.1109/TITS.2010.2053358

[10] Shao X, Naghdy F, and Du H. Reliable fuzzy H∞ control for active suspension of in-wheel motor driven electric vehicles with dynamic damping. Mech. Syst. Signal Process., 2017; 87: 365-383. https://doi.org/10.1016/j.ymssp.2016.10.032

[11] Nagarkar MP, Bhalerao YJ, Vikhe Patil GJ, and Zaware Patil RN. GA-based multi-objective optimization of active nonlinear quarter car suspension system-PID and fuzzy logic control. Int. J. Mech. Mater. Eng., 2018; 13(10). https://doi.org/10.1186/s40712-018-0096-8

[12] Han SY, Dong JF, Zhou J and Chen YH. Adaptive fuzzy PID control strategy for vehicle active suspension based on road evaluation. Electronics, 2022; 11(6) : 921. https://doi.org/10.3390/electronics11060921

[13] Gomonwattanapanich O, Pannucharoenwong N, Rattanadecho P, Echaroj S and Hemathulin S. Vibration control of vehicle by active suspension with LQG algorithm. International Journal of Automotive and Mechanical Engineering, 2020; 17(2): 8011-8018. https://doi.org/10.15282/ijame.17.2.2020.19.0600

[14] Quanser, Active Suspension System: User Manual, Quanser Corporation, Ontario, Canada, 2009.

[15] Manna S, Mani G, Ghildiyal S, Stonier AA, Peter G, Ganji V and Murugesan S. Ant colony optimization tuned closed-loop optimal control intended for vehicle active suspension system. IEEE Access, 2022; 10: 53735-53745. https://doi.org/10.1109/ACCESS.2022.3164522

[16] Fu Q, Wu J, Yu C, Feng T, Zhang N and Zhang J. Linear Quadratic Optimal Control with the Finite State for Suspension System. Machines, 2023; 11(2): 127. https://doi.org/10.3390/machines11020127

[17] Luhao W, Zhanshi S. LQR-Fuzzy control for double inverted pendulum. In 2010 International Conference on Digital Manufacturing & Automation, 1, 900-903, 2010. https://doi.org/10.1109/ICDMA.2010.170

[18] Hazem ZB, Fotuhi MJ and Bingül Z. A study of anti-swing fuzzy LQR control of a double serial link rotary pendulum. IETE Journal of Research, 2023; 69(6): 3443-3454. https://doi.org/10.1080/03772063.2021.1911690

[19] Welch G, Bishop G. An introduction to the Kalman filter, University of North Carolina, North Carolina, 1995.